In silico Medicinal Chemistry

Kooistra, A.J.

2015

document version
Publisher's PDF, also known as Version of record

Chapter 2

From three-dimensional GPCR structure to rational ligand discovery

Co-authored by: Rob Ieurs, Iwan J.P. de Esch, and Chris de Graaf
Published as: *Adv Exp Med Biol* 2014, *796*, 129-157.

Knowledge of the three-dimensional structure of G protein-coupled receptors (GPCRs) provides important insights into receptor function and receptor-ligand interactions. This information is key for the *in silico* rational discovery of new bioactive molecules that can target this family of pharmaceutically relevant drug targets.[114, 115] After the first GPCR crystal structure of bovine rhodopsin in 2000,[91] the first crystal structures of druggable GPCRs have been solved only in the past eight years[116] (see Chapter 1).[117] These GPCR crystal structures[116, 118] offer unique opportunities to push the limits of structure-based rational ligand discovery and design,[114, 116] and offer higher resolution templates for modeling the structures of GPCRs for which crystal structures have not yet been solved.[85, 118, 119] It should be noted, however, that modeling of GPCRs with low homology to the currently available GPCR crystal structures (e.g. class B[120-122] and class C GPCRs[123-125] as until recently only class A GPCR crystal structures were available) still remains a difficult task in which experimental data are of utmost importance to restrict the number of possible models.[115, 126] The challenges of GPCR modeling has been, for example, demonstrated in recent community wide competitions to predict GPCR crystal structures (GPCR DOCK 2008[127, 128], 2010[126, 129], and 2013[130]) and GPCR modeling methods have been described in several reviews.[115, 122, 131, 132] The current chapter gives an overview of the challenges and opportunities in structure-based discovery of GPCR ligands and focuses in particular on the developments in the period over the past 5 years in which the first druggable GPCR crystal structures have been used for rational GPCR ligand design. Different steps along the virtual screening workflow will be discussed in section 2. An overview of several successful structure-based ligand discovery studies in section 3 shows that GPCR models, despite structural inaccuracies, can be efficiently used to find novel ligands for GPCRs. Moreover, the recently solved GPCR crystal structures have further increased the opportunities in structure-based discovery of small molecule ligands for this pharmaceutically important protein family. All crystal structures clearly show the conserved heptahelical fold in the TM domain (Figure 2.1a) as well as for the intracellular helix 8.
The loops on the other hand differ highly between GPCRs in sequence composition, length, and (secondary) structure. Apart from that they have also shown to be harder to resolve in crystal structures as the electron density is distorted in this region, as is the case for ECL2 in, for example, the H_1R structure as well as some $A_{2A}R$ crystal structures. Within the conserved 7 TM helices and below the extracellular loops lies the conserved orthosteric binding site of GPCRs (Figure 2.1b) which can bind a plethora of different small molecules as well as peptides (Figure 2.1c).[72, 136]

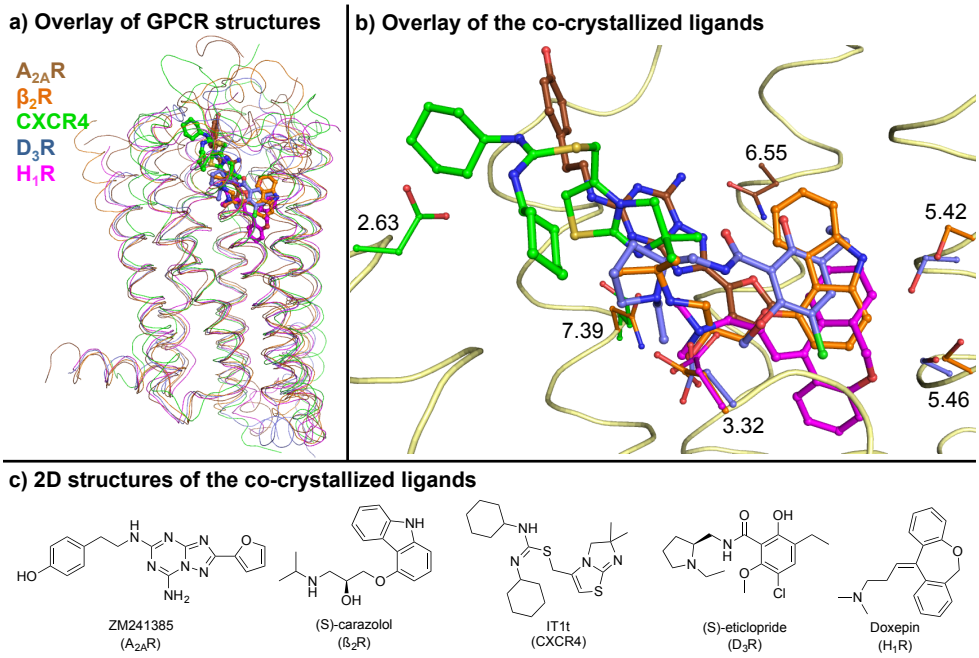

Figure 2.1 a) Structural alignment of multiple GPCR crystal structures (PDB-codes $A_{2A}R$:3EML,[133] β_2R:2RH1,[102] CXCR4:3ODU,[100] D_3R:3PBL,[134] H_1R:3RZE[90]) highlight the highly conserved TM fold b) Close-up of the co-crystallized ligands within the conserved binding site. The backbone of carazolol bound β_2R (PDB-code: 2RH1[135]) is depicted as a light yellow ribbon. Residue positions are indicated using the Ballesteros Weinstein numbering scheme[83] and both the ligands and selected residues are colored according to the coloring scheme depicted in a. c) 2D structures of the co-crystallized ligands depicted in b.

2.1 Hierarchical workflow for GPCR structure-based ligand discovery

This section will describe the steps along a hierarchical virtual screening workflow applied in many GPCR virtual screening studies (Figure 2.2). Although the different steps can be generally applied to other protein targets, it should be noted that incorporation of target specific information can highly increase the chance on success. In step 1 the initial compound library[137] can be filtered to remove undesirable compounds that contain chemical moieties that can interfere with experimental validation assays by forming aggregates, chemically reacting with proteins or directly interfere in assay signaling.[138] Furthermore one can decide to exclude compounds that contain scaffolds associated with toxicity[139] or that have poor oral bioavailability[140]. In most reported GPCR-based virtual screening studies, such pre-filters are applied to construct the chemical library to be screened (Table 2.1). Additional filters, based on the properties (e.g. molecular weight, number of rotatable bonds, number of rings, hydrogen bond donor/acceptor counts, number of positively/negatively charged atoms, etc.) of a set of known actives (step 1 of Figure 2.2), are applied in most GPCR VS studies as well (Table 2.1) to obtain a more focused chemical database. Substructures,[141-144] chemical similarity descriptors,[143, 145, 146] and 3D-shape similarity or pharmacophore models[122, 141, 143, 145, 147] (Table 2.2) derived from known ligands can be used to narrow down the number of compounds to be handled during conformational sampling (step 2) even further. These methods can also be used inversely in order to limit the focused database to

novel ligands, i.e. small molecules that have a low similarity (as assessed by the applied method) compared to known ligands (available in target annotated chemical databases like WomBat[148], BindingDB[57] and ChEMBL[54]). However, more often such novelty filters are applied after docking the compounds in the database (although computationally more expensive).

In step 2 the chemical database is automatically docked in the receptor model. Many different automated docking programs and scoring functions based on different physicochemical approximations are available[149] (section 2.2). In some GPCR SBVS studies docking based screening simulations have been guided by pharmacophore constraints.[143, 147, 150] Pharmacophore models and/or exclusion constraints derived from structural models of receptor-ligand complexes (or the receptor alone) can be used as an alternative structure-based virtual screening approach to molecular docking simulations, as demonstrated in several successful GPCR SBVS campaigns to discover ligands of C3aR,[151] CB_2R,[152] FFAR1,[146] FPR1R,[153] MCHR1,[145] H_3R.[150]

In step 3, the docking poses are post-processed and ranked. Many SBVS investigations have only employed docking scoring functions to rank docking poses, but more and more structure-based *in silico* screening protocols include additional filters to post-process docking results (section 2), because the scoring accuracy of docking-scoring combinations is very much dependent on physicochemical details of target-ligand interactions and fine details of the protein structure. Strategies to overcome these problems are: i) the use of consensus scoring strategies,[147, 154-156] ii) topological filters to filter out poses exhibiting steric or electrostatic mismatches between the ligand and the binding site,[122] iii) receptor-ligand interaction *post*-processing filters[157-159] (Tables 1-2) and/or iv) receptor-ligand interaction fingerprint (IFP) scoring methods to select and rank poses based on binding mode similarity with reference ligand poses[115, 122, 160-162] (section 2, Figure 2.4 and 5).

Before selecting the final compounds (step 4), the novelty of the discovered hits can be assessed by 2D or 3D similarity searches against previously known ligands (as discussed earlier), as performed in recent virtual screening studies against e.g. $A_{2A}R$,[158, 163] β_2R,[164] D_3R,[157] and H_1R[161] (Table 2.2). Moreover, 2D and 3D ligand-based similarity searches of the screening database against the reference ligand used to refine the receptor (or present in the receptor co-crystal structure) can be performed to demonstrate the strength of the SBVS approach.[122, 161] When too many ligands are retrieved along the VS funnel, it is generally wise to cluster virtual hits by chemical diversity before visual inspection. Compounds can be classified by their chemical scaffold in order to prioritize scaffolds rather than individual compounds in screening ranking lists. Sampling a few representative analogues for each scaffold usually enables a selection of chemically dissimilar compounds for biological evaluation.[144] Finally, the selected docking poses and compounds should be visually inspected in step 4 for the ultimate selection: no algorithm yet outperforms the brain of an experienced modeler for such a task.

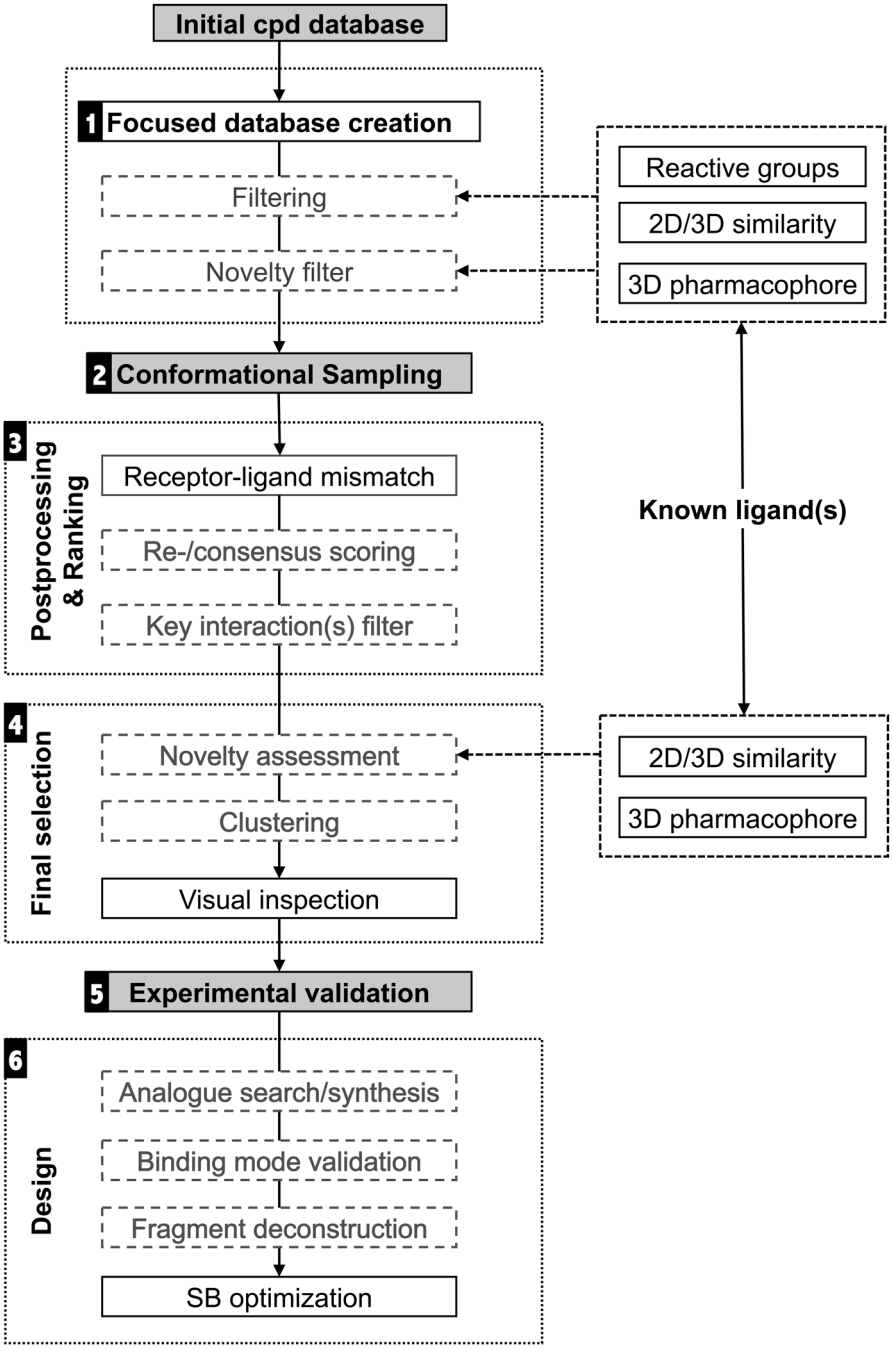

Figure 2.2 Structure-based virtual screening (SBVS) workflow (see section 2 for description of the individual steps, section 3 and Tables 1-2 for details of SBVS runs against specific GPCRs, and section 4 for the discussion of step 6 observed in reported SBVS studies).

Although this chapter mainly focuses on SBVS studies (and primarily docking-based virtual screening campaigns) it should be noted, however, that there are alternative (or complementary) screening methods that have been successfully applied for the discovery of novel ligands (e.g. ligand-based similarity (2D and 3D), and receptor/ligand-based pharmacophore searches[144-146, 151-153]). For 3D similarity and receptor-based pharmacophore searches the receptor-bound conformation of reference compounds can be derived from docking simulations in the receptor model. The obtained receptor-ligand complexes are used to derive the information for the 3D-similarity searches or the creation of pharmacophore models. Alternatively, pure receptor-based pharmacophore models, extracted from ligand-receptor interaction hot spots in the binding pocket, can be used even in the absence of a ligand,[31, 34, 165] as successfully applied for the discovery of C3aR ligands (incl. 45).[151] Frequently GPCR homology model-based virtual screening studies combine multiple screening methods and filtering steps into a hierarchical workflow. In general, large chemical database are first filtered by application of a 2D and/or 3D pharmacophore model after which the focused library is subjected to molecular docking simulations (Table 2.1, Figure 2.1). This type of hierarchical SBVS has frequently been applied to bRho-based homology models in order to find novel ligands.[115] Apart from the hierarchical approach also integrated approaches are known in which pharmacophore constraints guide the conformational sampling of docking simulations, as applied in virtual screening campaigns against α_{1A}-adrenoceptor[147] and NK_1R.[143] In general the more recent crystal structure-based SBVS campaigns do not apply ligand-based pharmacophores but instead use physicochemical property filters (e.g. heavy atom count, number of rings, hydrophobicity) and emphasize experimentally supported receptor-ligand interactions (e.g. the essential ionic interaction with $D107^{3.32}$ for H_1R[161]) to score and select docking poses (Tables 1-2).

After these final steps of the virtual screening process a highly diminished subset of the original compound database (typically between 0.001% and 0.05 % of the original database, Table 2.1) is obtained and their (commercial) availability is checked. The available compounds are subsequently obtained and experimentally validated (step 5). Many times the experimentally validated hits of these virtual screening studies are not further investigated, however, more and more often the hits are only a starting point and used for further (structure-based) optimization (step 6, section 4).

Table 2.1 Overview of prospective structure-based virtual screening (SBVS) against GPCR models and crystal structures since 2009.[a] See de Graaf and Rognan[115] for an overview of successful prospective GPCR structure-based virtual screening campaigns before 2009 (comprising campaigns against bioaminergic, brain-gut peptide, chemokine, lipid, peptide, and purine receptors).

Receptor[b]	Template	Focused database creation[c]	Conf. Sampling[d]	(Re)scoring[e]	Interaction filter[f]	Prospective initial db[g]	Prediction hits[h] (tested)	Ref [i]
Adenosines								
A_1R	$A_{2A}R$	II	ad	score	$N^{6.55}$	2 200 000	8 ant (39)	166
$A_{2A}R$	X-ray	dl	ad	LE/chem/ score	-	4 300 000	23 ant (56)	163
$A_{2A}R$	X-ray	CNS+dl	ad	score	$N^{6.55}$+$E^{45.53}$	1 400 000	7 ant (20)	158
$A_{2A}R$	β_1R	dl	ad	score[m]	$N^{6.55}$	545 000	20 lig (230)	159, 167, 168
Amines								
5-$HT_{2A}R$	β_2R	fda	ad	rescoring	D3.32	1430	1 lig (6)	169
β_2R	X-ray	dl	ad	clust+-score[m]	$D^{3.32}$	1 000 0000	6 ant (25)	164
D_3R	β_1R/2	dl	ad	score[m]	$D^{3.32}$+$S^{5.43+5.46}$	3 300 000	6 ant (26)	157
D_3R	X-ray	dl	ad	score[m]	$D^{3.32}$+$S^{5.43+5.46}$	3 300 000	5 ant (25)	157
H_1R	H_1R	fl	ad	score+IFP	$D^{3.32}$	108 790	19 ant (26)	161
H_3R	H_1R	fl	3D	score (SB+LB)	$D^{3.32}$	771 219	18 lig (29)	150
H_4R	ADRB	fl	ad	IFP	$D^{3.32}$	43 326	6 lig (23)	170
Chemoattractants								
OXER	CXCR4	fl	ad	score	-	1047	1 lig (10)	171
Chemokines								
CXCR4	de novo	none	ad	Score	$D^{4.60}$/$D^{6.58}$/ $E^{7.39}$	350 000	1 ant (32)	172
CXCR4	bRho β_1R β_2R $A_{2A}R$	II	ad	Score	$E^{7.39}$	3 300 000	1 lig (24)	173
CXCR4	X-ray	II	ad	Score	$E^{7.39}$	4 200 000	4 lig (23)	173
Lipids								
CB_2R	β_2R	fl	2D+ad	Score	$S^{7.39}$	250 675	13 lig (97)	174
Peptides								
C3aR	AT1R	none	3D	clust.	-	in-house	4 ago (157)	151
Purines								
$P2Y_1R$	bRho	3D+clust	3D	3D+clust.		250 675	3 lig (110)	175
Secretin								
GLR	CRFR1	II(+3D)	ad	score + IFP	$K^{2.53}$	1 900 000	3 lig (26)	122

[a] Only structure-based virtual screening studies targeting the TM domain are included, [b] Receptors are clustered according to Surgand et al. [72]; [c] Consecutive filters (dl (drug-like physicochemical properties), ll (lead-like physicochemical properties), fl (fragment-like physicochemical properties), 1D (physicochemical properties known ligands), 2D (two-dimensional topological/chemical similarity/pharmacophoric features/sub groups), 3D (three-dimensional pharmacophore)) used to compile database for docking/3D conformer search; [d] Conformer search method: ((H-bond) constr(ained)) automated docking (ad), protein-based or docked ligand-based 3D pharmacophore search (3D); [e] Method to score, rank and/or filter conformers: clust. (scaffold clustering), (c-)score ((consensus) docking scoring function), 2D (two-dimensional topological/chemical

similarity/pharmacophore features/sub-groups), 3D (three-dimensional pharmacophore); [f] Key interactions with the listed residues were used to filter the docking poses; [g] Prospective validation: initial database (db) and [h] number of experimentally confirmed hits with detectable affinity/activity (of the total number of tested compounds); [i] References to homology modeling, virtual screening, and structure-based ligand optimization studies are provided.

2.2 *In silico* Structure-based GPCR Ligand Discovery

The recent crystal structure determinations of druggable GPCRs[176] have now opened up excellent new opportunities to push forward the limit of crystal structure-based GPCR ligand discovery.[157-159, 161, 163, 164, 177, 178] It should be noted, however, that despite their possible structural inaccuracies GPCR homology models can also be (and have been) efficiently used to find new ligands.[122, 141, 143-147, 150-153, 157, 159, 161, 166, 169-175, 179-181] Moreover, the new GPCR crystal structures allow for the creation of higher resolution homology models as more templates are available.

As described in section 2, many of the reported GPCR structure-based SBVS campaigns included a customized hierarchical virtual screening workflow. Table 2.1 gives an overview of recent prospective structure-based VS studies against GPCR models (since our review of 2009[115]). Table 2.2 presents the molecular structures of representative agonists as well as antagonists identified by prospective SBVS studies in GPCR models and crystal structures. Figure 2.3 shows the hit rates, ligand efficiency and size of experimentally validated hits in these *in silico* screening campaigns. It should be noticed that SBVS often yields new chemical scaffolds (Table 2.2) that still contain essential functional groups like positively or negatively charged atoms that are used as substructure or pharmacophore filters/constraints to set up the initial ligand database or score/rank docking poses (Table 2.1). Most of the *in silico* screening studies have focused on bioaminergic receptors,[141, 147, 157, 161, 164, 179] but several successful prospective SBVS campaigns are reported also for other rhodopsin-like GPCRs (adenosine[158, 159, 163], brain-gut peptide[145, 180], chemoattractant[171], chemokine[144, 172, 179, 181], lipid[152], peptide[143, 151, 153], purine receptors[146]). More recently the first prospective (homology model-based) SBVS studies targeting the allosteric TM cavity of class B GPCRs has been reported[122] and SBVS studies against class C GPCRs have so far only focused on the orthosteric N-terminal binding site (Venus Fly trap[182]). This will probably change quickly as in the past year the first crystal structures of class B, C, and F (Frizzled) GPCRs have become available (chapter 1). The final section will discuss one of the important next steps after a SBVS for GPCR ligands, namely the *structure-based optimization* of virtual screening hits (section 4).

SBVS campaigns against the first crystal structures of druggable GPCRs (β_2R, A_{2A}R, DRDR3, and H_1R) have resulted in relatively high hit rates (Figure 2.3, up to 73% hit rate [161]). It should be noticed, however, that high hit rates have not only been obtained based on docking studies against GPCR crystal structures, but also successful SBVS studies with high hit rates (>20%) have been reported based on GPCR homology models (Figure 2.3) [141, 147]. Moreover, in a recent comparative virtual screening comparable high hit rates were obtained for prospective virtual screening runs against the recently solved dopamine D_3 receptor (D_3R) crystal structure and a previously constructed D_3R homology model [157]. A different result was obtained in a comparative CXCR4 SBVS study in which the screen against the CXCR4 crystal structure was more successful. SBVS studies using homology models are highly dependent on the applied method as well as the homology model used as was recently demonstrated by Kolb et al. [166] who created four A_1R homology models with highly varying hit-rates.

The first crystal structure-based virtual screening study for a druggable GPCR was reported for β_2R.[102] Kolb et al.[164] performed docking simulations of 972 608 lead-like compounds against the β_2R crystal structure. They selected 25 compounds for experimental testing from the 500 top-ranking molecules based on chemical clustering, visual inspection, and favorable interaction energies with $D^{3.32}$ (Tables 1-2). 6 of the 25 hits had detectable binding affinity for β_2R (K_i values ranging from 4 to 0.009 μM) and were characterized as inverse agonists. Interestingly, the predicted binding mode of the highest affinity hit **19** (Table 2.2), was later corroborated by crystallization studies. Although this is not unexpected given its chemical similarity to the reference ligand used (carazolol, **18**), this demonstrates that GPCR structure-based virtual screening can not only yield new ligands, but also suitable starting points for structure-based hit optimization. Also several chemically novel β_2R ligands were reported (e.g. cpd. **21**), which is particularly challenging for β_2R, a receptor with a relatively low ligand diversity.[183] In fact, in 2008 Topiol et al. discovered several submicromolar affinity ligands based on the β_2R crystal structure that were chemically very close to known β_2R ligands.[177, 178]

The β_2R crystal structure has been used in several studies as a template for the creation of homology models. Istyastono et al., for example, used the β_2R structure to generate JNJ7777120 (cpd. **30**) and VUF10497 (cpd. **31**) bound H_4R homology models.[170] These models were subsequently used for VS purposes. 23 112 fragment-like molecules were obtained from the ZINC database after filtering out the compounds containing reactive groups. After docking all compounds, the highest-ranking (according to the IFP score) and novel (according to their low 2D similarity to known H_4R ligands from the ChEMBL) compounds were selected and clustered using a 2D ligand-based fingerprint. From each cluster the top compound was selected and in total 164 compounds were remaining for visual inspection. During the visual inspection compounds with an ionic interaction with $D^{3.32}$ and a polar moiety near $E^{5.46}$ were prioritized resulting in the purchase of 23 compounds. 6 of the 23 compounds (including hits **32** and **33**) were shown to have affinities in the range of 0.14 to 6.3 μM.[170]

Two successful docking-based virtual screening studies against the A_{2A}R crystal structure have been performed,[158, 163] yielding diverse sets of novel ligands (**6-8**, **9a**, **10a**, Table 2.2). Katritch et al. selected 56 high ranking compounds from docking based virtual screening runs of 4 million compounds against the A_{2A}R crystal structure and discovered 23 new A_{2A}R ligands with K_i values between 0.032 and 10 μM (incl. **6**, **7**).[163] Interestingly, specific water molecules in the A_{2A}R binding site were included in the docking simulations, because retrospective virtual screening evaluations gave better results with than without consideration of water.[163] Carlsson et al. emphasized favorable H-bond interactions with $N^{6.55}$, an important A_{2A}R ligand binding residue,[184-186] in their scoring protocol to rank the docking poses of 1.4 million compounds in the A_{2A}R crystal structure by increasing the dipole moment of the side chain amide group, but without taking water into account.[158] Using this experimentally guided SBVS approach, 7 of the 20 selected hits were experimentally confirmed as novel A_{2A}R ligands, with K_i values ranging from 0.2 to 9 μM (incl. **8**).[158] Recently an β_1R-based A_{2A}R homology model[186] (that correctly predicted the binding mode of ZM241385 prior to publication of the A_{2A}R-ZM243185 crystal structure[133]) was successfully used to discover new A_{2A}R ligands.[159] The overall hit rate of this *in silico* screening campaign was somewhat lower than the A_{2A}R crystal structure-based screening runs (Figure 2.3), but yielded a diverse set of chemically novel ligands (e.g. **9a**, **10a**)[159] that were subsequently optimized by structure-based design to improve affinity and adenosine receptor selectivity (section 4).[159, 167] Both receptor model construction as ligand optimization was driven by experimental (mutagen-

esis/biophysical mapping[186] of receptor-ligand interaction hotspots) and computational analysis (identification of thermodynamically unstable water molecules that can be displaced by the ligand).[159, 167, 168]

With the antagonist bound $A_{2A}R$ crystal structure as a template, Costanzi et al.[175] created a homology model of the $P2Y_1$ receptor ($P2Y_1R$). The ligand and receptor based pharmacophore screen was performed on a set of 133 999 compounds that were selected from a set of 250 675 compounds using physicochemical filtering. The resulting 362 hit compounds were subsequently clustered and from each cluster one unique compound was selected. The resulting 110 compounds were subsequently validated *in vitro* for their binding affinity for $P2Y_1R$, yielding multiple hits (the exact number was not reported). One of the hit compounds (with a reported binding affinity of 13 μM) was further explored through use of an analogue search and SAR studies (section 4). This work resulted in new insights in the binding mode properties of this non-nucleotide $P2Y_1R$ antagonist series.[175]

Carlsson et al. compared the SBVS performance of the dopamine D3 receptor (D_3R) crystal structure and an β_2R-based homology model of D_3R (that was constructed prior to the release of the D_3R X-ray structure).[157] 26 and 25 of the highest ranking molecules with strong electrostatic interactions with $D^{3.32}$ (Tables 1-2) were selected for experimental testing from 2.3 million molecules docked in the D_3R homology model and D_3R crystal structure, respectively. Interestingly, both models performed equally well in terms of virtual screening hit rate (Figure 2.3). 6 of the homology model-based hits had affinities ranging from 0.2 to 2.1 μM (incl. hits **15**, **16**, **17a**, Table 2.2), while 5 of the X-ray structure-based hits had affinities ranging from 0.3 to 2.0 μM (incl. hits **13**, **14**). Ligand **17** from the homology model screen was optimized to improve affinity (81 nM, section 4) [157].

A customized structure-based virtual screening protocol against the histamine H_1 receptor (H_1R) crystal structure was used to dock and score a database of 108 790 fragment-like compounds (heavy atoms ≤ 22) containing a basic moiety (Chapter 4). The method combined molecular docking simulations with a protein-ligand interaction fingerprint (IFP) scoring method (Figure 2.4). The optimized *in silico* screening approach was successfully applied to identify a chemically diverse set of novel fragment-like (≤22 heavy atoms) H_1R ligands with an exceptionally high hit rate of 73%. Of the 26 tested fragments, 19 compounds had affinities ranging from 10 μM to 6 nM (incl. hits **23-25**) This study shows the potential of *in silico* screening against GPCR crystal structures to explore novel, fragment-like GPCR ligand space.[161]

The H_1R crystal structure also allowed Sirci et al. to create high-resolution homology models of H_3R.[150] Multiple MD snapshots of the homology models were subjected to retrospective validation using the experimental data from a VU-MedChem fragment library screen against H_3R. The snapshot with the highest early enrichment was selected from both the methimepip-based (cpd. **26**) and the VUF5228-based homology model. After a retrospective comparison of both models using docking and FLAP-linear discriminant analysis (FLAP-LDA), the latter in combination with the methimepip-based homology model was shown to be superior in the retrieval of active fragment-like compounds. Multiple different ligand-based FLAP models were build (based on amongst others reference compound **27**) in parallel as well, and were also retrospectively validated. Subsequently a prospective screening of 156 090 fragment-like compounds against both the best structure-based and ligand-based FLAP-LDA models was performed. From the highest scoring compounds for both the ligand *and* structure-based model 21 compounds were purchased as well as 8 from the highest scoring compounds from only the ligand-based model.

Experimental validation pointed out a remarkably high hit rate of 62% as 18 of the 29 selected compounds were found to be active. This study showed that the combined use of ligand-based and structure-based models with a thorough retrospective validation can be the key to a successful VS.[150]

Mysinger et al. used a chemokine receptor CXCR4 crystal structure and a CXCR4 homology model (constructed before the release of the crystal structure) in a comparative virtual screening study.[173] 2.3 and 4.2 million lead-like compounds were docked against the homology model and crystal structure respectively. The binding modes of the top 500 compounds from each screen were visually inspected. Based on availability, internal energy, unsatisfied polar interactions, correctness of the protonation state and hit diversity 24 and 23 compounds were selected for the crystal structure and homology model screening respectively. Experimental validation yielded 1 and 4 hit compounds (a hit rate of 4% and 17%) respectively and showed affinities ranging from 0.31 μM (hit **41**) to 225 μM (hit **40**). This study underlined the impact of the available templates and experimental knowledge for the creation of homology models.[173]

Kim et al.[172] constructed a CXCR4 homology model based on binding mode of AMD3100 (cpd. **38**), and validated this model using published site-directed mutagenesis data. 350 000 compounds from the open NCI database were docked in three conformations of the homology model. From the docked compounds the neutral molecules with a buried surface area of at least 80% in close proximity to the acidic residues $D^{4.60}$, $D^{6.58}$ and $E^{7.39}$ were selected, excluding 90% of the small molecules. For the remaining molecules the binding energies were calculated and the top 200 compounds in each receptor conformation were visually inspected, resulting in a subset of 50 compounds of which 32 were procured and experimentally validated. One hit was obtained (cpd. **39a**) which was further investigated because of its close similarity to known anti-malarial drugs (section 4).[172]

Blätterman et al.[171] used the CXCR4 crystal structure [100] to construct a homology model of an oxoeicosanoid receptor 1 (OXER) homology model. Commercially available compounds from the ZINC database were filtered based on physicochemical properties, resulting in a subset of 1047 compounds. This subset was docked into the OXER homology model and from the top 100 (as ranked by AutoDock), 10 compounds were visually selected and tested for OXER mediated Ca^{2+} release-inhibition. One of the 10 compounds (hit **43**) showed significant inhibition and was further investigated. Ligand deconstruction of this hit compound yielded no substructures with any binding affinity for OXER implying that the complete molecule, as discovered, was needed in order to successfully bind to OXER and inhibit the CA^{2+} flux. Further functional assays highlighted that this compound was biased and inhibited Gβγ but not Gαi signaling.[171]

The work by Kolb et al.[166] discussed earlier pushed the boundaries of virtual screening as they tried to screen for subtype selective ligands and evaluate the impact of homology model inaccuracies/differences. Four different A_1R homology models based were created based on the antagonist bound $A_{2A}R$ crystal structure. These models were subjected to docking simulations of 2.2 million lead-like compounds from the ZINC database. Within this docking simulation the conserved interaction with $N254^{6.55}$ was accentuated by amplifying this term. The top 500 of the docking results from each of the models was inspected to filter out molecules with unsatisfied hydrogen bond donors and acceptors, incorrect protonation states, unlikely binding modes or highly strained conformation which resulted in the purchase of 39 compounds in total. All 39 compounds were tested for their A_1R, $A_{2A}R$ and A_3R affinity in order to assess their selectivity. 8 of the compounds showed activity for the A_1R receptor (incl. hits **3** and **4**), but surprisingly,

15 and 14 compounds were active on the $A_{2A}R$ and A_3R, respectively. In total 20 of the 39 compounds were active on one (or more) of these three receptors. Interestingly, not all homology models performed equally well; one of the models did not yield any hits and another model accounted for half of the active compounds (but only one of the A_1R active compounds, namely hit **3**). This study highlighted once more the effect of small structural differences in the receptor model or crystal structure on virtual screening, and the challenges in virtual screening for receptor subtype selective ligands.

Virtual screening studies can also highlight surprising cross-pharmacology as was demonstrated in the VS study by Lin et al.[169] A 5-$HT_{2A}R$ homology model was created based on the timolol bound β_2R crystal structure.[187] Using MD, 10 induced-fit models for both ketanserin- and cyproheptadine-bound 5-$HT_{2A}R$ were generated. These 20 snapshots were subsequently used to include protein flexibility and afterwards subjected to a retrospective validation. The ketanserin (cpd. **34**) and cyproheptadine (cpd. **35**) bound models with the best early enrichment were selected for a prospective screening study. A filtered ($100 \leq MW \leq 600$) compound library, comprising 1430 FDA approved drugs, was screened against the two models using docking and a MM-GB/SA refinement and rescoring procedure. The top 200 hits were filtered based on an essential hydrogen bond filter with $D^{3.32}$ and chemical novelty assessment based on comparisons with known 5-$HT_{2A}R$ ligands in ChEMBL[54] and DrugBank[55] and SEA predictions.[188] Of the 6 compounds that were selected for experimental validation, the kinase inhibitor sorafenib (hit **36**) showed a binding affinity of 1959 nM for 5-$HT_{2A}R$. This compound **36** was also tested on the other HT receptor subtypes and found to be active against all with an affinity ranging from 56 to 7071 nM. It should be noted that although sorafenib is not able to form the conserved salt bridge with $D^{3.32}$, the urea moiety of sorafenib is seemingly able to provide a strong hydrogen bond to $D^{3.32}$ thereby replacing the necessity for a basic moiety.

Renault et al.[174] used a combined approach of a trained ligand-based filter and an automated docking approach for the identification of novel ligands for the cannabinoid receptor 2 (CB_2R). A database of 5 513 820 compounds was reduced using physicochemical filtering resulting to a subset of 3 495 595 compounds. This dataset was subjected to a trained 2D-based Bayesian classifier (based on 90 compounds with measured affinity for CB_2R) that further reduced the compound set to 209 442 compounds. Docking in an active-state CB_2R homology model (using carazolol-bound (cpd. **18**) inactive-state β_2R[102] as a template) with an interaction filter on $S^{7.39}$ resulted in the selection of 1385 compounds of which 150 were selected and 149 were available for purchase. Due to solvation issues only 97 of the compounds could be tested which resulted in the confirmation of 13 hits with affinities ranging from 2.3 nM (hit **47**) to 71 μM.

De Graaf et al.[122] constructed a homology model of the glucagon receptor (GLR), a class B GPCR, based on a validated structural model of the CRFR1 receptor. For this representative class B GPCR numerous experimental ligand and receptor data were available to guide the modeling procedure and to validate the refined model with retrospective virtual screening studies (see section 2). A database of 1.9 million commercially available drug-like compounds was screened for chemical similarity to existing GLR noncompetitive antagonists and docked to the transmembrane cavity of the GLR homology model. 23 compounds were selected based on binding mode similarity to the protein-ligand interaction fingerprints of the docking poses of two different reference ligands (known GLR ligands **65** and L-168 049) in the GLR homology model. Two of the 23 compounds inhibited the effect of glucagon in a dose-dependent manner (both from the hit list ranked according to IFP similarity to the reference binding mode of **50**). Interestingly, one *in*

silico hit that was inactive at the GLR was shown to bind to GLP-1R and potentiate the response to the endogenous GLP-1 ligand. This illustrates the strength of using two alternative binding mode hypotheses in prospective SBVS studies. Although the potencies of the ligands are still modest, this study showed for the first time that structure-based approaches can indeed be used to identify novel class B non-competitive ligands.[122]

Table 2.2 Representative ligands obtained in structure-based virtual screening (and design) studies against GPCR homology models and X-ray structures.

A_1R (model)[166]			
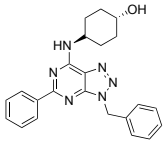	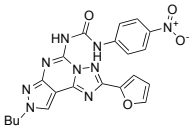	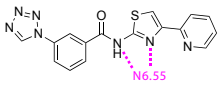	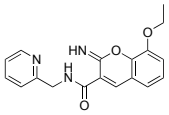
1 (ref)	**2 (ref)**	**3**	**4**
pK_i = 8.5 (ant)	pK_i = 6.2 (ant)	pK_i = 5.5 (ant) * not active on A2A	pK_i = 6.4 (ant)* $\Delta pK_{i,\ A1\text{-}A2A}$ = 0.3
$A_{2A}R$ (model/X-ray)			
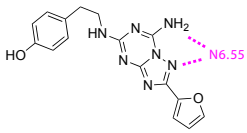	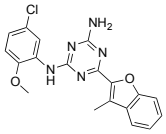	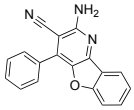	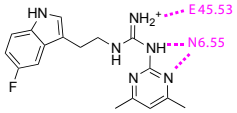
5 (ref)[158, 163]	**6**[163]	**7**[163]	**8**[158]
pK_i = 9.0 (ant)	pK_i = 7.5 (ant)*	pK_i = 7.5 (ant)*	pK_i = 6.7 (ant)*
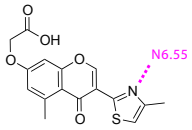	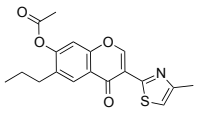	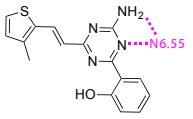	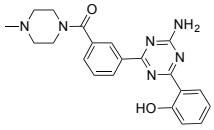
9a[159]	**9b**[159]	**10a**[159]	**10b**[159]
pK_i = 5.7 (ant) -	pK_i = 8.5 (ant) $\Delta pK_{i,\ A2A\text{-}A1}$ = 1.2	pK_i = 8.5 (ant) $\Delta pK_{i,\ A2A\text{-}A1}$ = 1	pK_i = 9.0 (ant) $\Delta pK_{i,\ A2A\text{-}A1}$ = 1.8
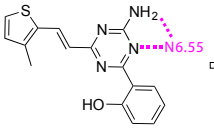	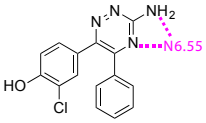	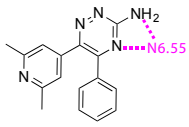	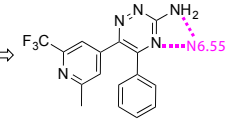
10a[159]	**11a**[167]	**11b**[167]	**11c**[167]
pK_i = 8.5 (ant) $\Delta pK_{i,\ A2A\text{-}A1}$ = 1	pK_i = 8.9 (ant) $\Delta pK_{i,\ A2A\text{-}A1}$ = -0.9	pK_i = 8.1 (ant) $\Delta pK_{i,\ A2A\text{-}A1}$ = 1	pK_i = 8.5 (ant) $\Delta pK_{i,\ A2A\text{-}A1}$ = 1

D_3R (model/X-ray)[157]

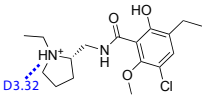

12 (ref)
pK_i = 9.7 (ant)*

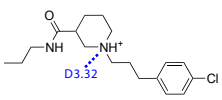

13
pK_i = 6.5 (ant)*

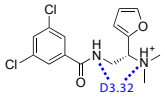

14
pK_i = 5.7 (ant)*

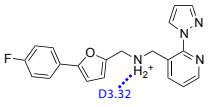

15
pK_i = 5.9 (ant)*

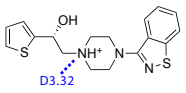

16
pK_i = 6.7 (ant)*

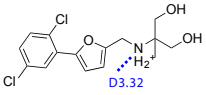

17a
pK_i = 5.8 (ant)*

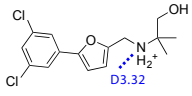

17b
pK_i = 7.1 (ant)*

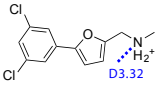

17c
pK_i = 7.0 (ant)*

β_2R (X-ray)[164]

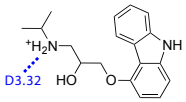

18 (ref)
pK_i = 10.0 (ant)

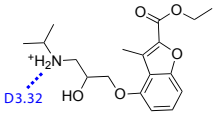

19
pK_i = 8.0 (ant)*

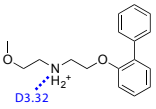

20
pK_i = 6.3 (ant)

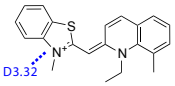

21
pK_i = 6.0 (ant)*

H_1R (X-ray)[161]

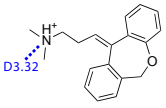

22 (ref)
pK_i = 9.7 (ant)

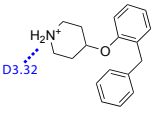

23
pK_i = 8.2 (ant)*

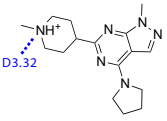

24
pK_i = 7.2 (ant)*

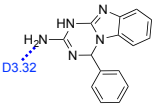

25
pK_i = 6.4 (ant)*

H_3R (model)[150]

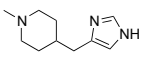

26 (ref)
pK_i = 9.0 (ago)

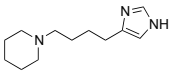

27 (ref)
pK_i = 7.7 (ago)

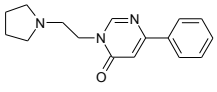

28
pK_i = 5.9

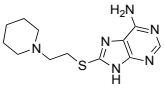

29
pK_i = 5.9

H_4R (model)[170]

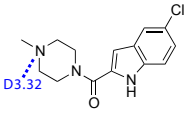

30 (ref)
pK_i = 7.8 (biased ago)

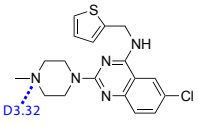

31
pK_i = 8.1 (ant)

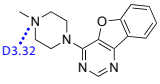

32
pK_i = 6.9

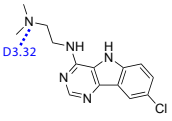

33
pK_i = 5.2 (ant)*

5HT2A (model)[169]

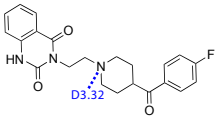

34 (ref)
pK_i = 8.5 (ant)

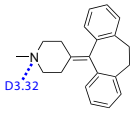

35 (ref)
pK_i = 9.3 (ant)*

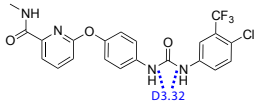

36
pK_i = 7.3

CXCR4 (model/X-ray)[169]

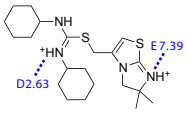

37 (ref)[173]
pIC_{50} = 8.1

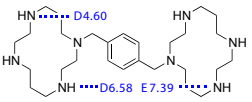

38 (ref)[172]
pIC_{50} = 7.2 (ant)

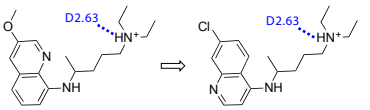

39a[172]
pIC_{50} = 5.3 (ant)

39b (analogue)[172]
pIC_{50} = 5.2 (ant)*

OXER (model)[171]

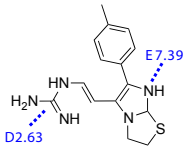

40[173]
pIC_{50} = 2.6 (ant)

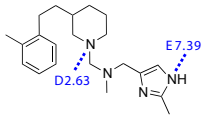

41[173]
pIC_{50} = 6.5 (ant)*

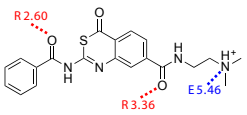

42 (ref)
- (biased ago)

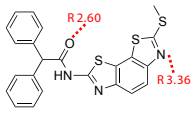

43
- (biased ant)

C3aR (model)[151]

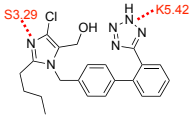

44 (ref)
pEC_{50} (AT_1) = 8.1 (ago)

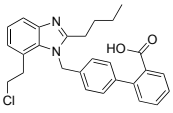

45
pEC_{50} = 6.5 (ago)

CB_2R (model)[189]

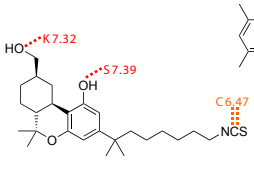

46 (ref)
pEC_{50} = 9.0 (ago)

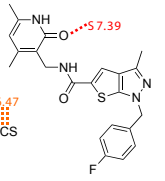

47
pEC_{50} = 8.5 (ago)

$P2Y_1R$ (model)[175]

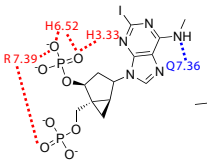

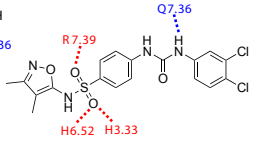

48 (ref)
pK_i = 9.0 (ant)

49
pK_i = 4.9 (ant)

GLR (model)[122]

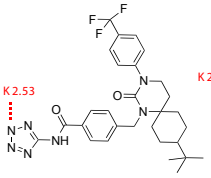

50 (ref)
pIC_{50} = 7.5 (ant)

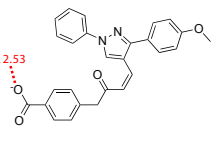

51
pIC_{50} = 4.6 (ant)*

H-bond donor/positive ionizable (blue), H-bond acceptor/negatively ionizable (red) or both (magenta) pharmacophore features (assigned to functional groups in the ligands) and docking constraints/post-processing interaction filters (indicated by dotted lines to complementary residue(s) in the receptor) are derived from reference ligands/binding modes and used to select hits along the virtual screening work flow (Figure 2.2, Table 2.1). The experimentally determined affinity/activity parameters and function (full/partial agonist (ago) and/or inverse agonist/antagonist (ant)) of reference and discovered ligands are indicated. Homology model-based and crystal structure-based virtual screening reference compounds as well as hits are highlighted in blue and red respectively. [a)] Analogue of SBVS hit: known antimalarial drug chloroquine. [*)] Novelty of the hit was explicitly assessed.

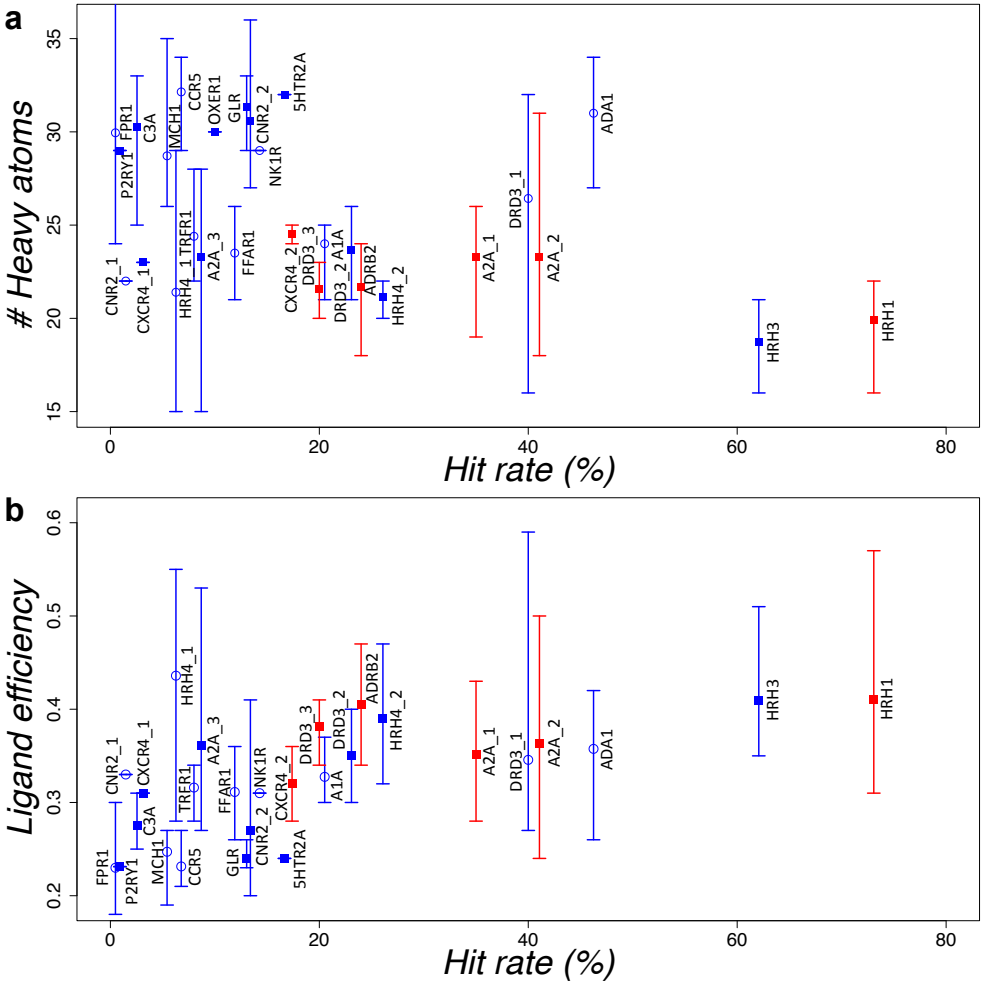

Figure 2.3 Hit rate versus size (heavy atom count) (a) and hit rate versus ligand efficiency (b) of hits identified in prospective structure-based virtual screening studies against GPCR crystal structures (red) and homology models (blue). Open circles indicate a SBVS studies published before 2009, studies since 2009 are indicated with a closed square. The bars shown indicate the minimum and maximum heavy atom and ligand efficiency count for all hits of each SBVS respectively. The labels indicate the screening on the following receptors adenosine A_1 (A1A), adenosine A_{2A} receptor (A2A_1[158], A2A_2[163], A2A_3[159]), adrenergic α_{1A} receptor (ADA1[147]), adrenergic β_2 receptor (β_2R[164]), complement component 3a receptor 1 (C3A[151]), C-C chemokine receptor type 5 (CCR5[144]), cannabinoid receptor 2 (CNR2_1[152], CNR2_2[174]), chemokine receptor CXCR4(CXCR4_1[172], CXCR4_2[173]), dopamine receptor D_3 (DRD3_1[141] and DRD3_2[157] and DRD3_3[157]), free fatty acid receptor 1 (FFAR1[146]), formyl peptide receptor 1 (FPR1[153]), glucagon receptor (GLR[122]), histamine receptor H_1 (HRH1[161]), histamine receptor H_3 (HRH3[150]), histamine receptor H_4 (HRH4_1[156], HRH4_2[170]), 5-hydroxytryptamine receptor 2A (5-HT_{2A}R[169]), melanin-concentrating hormone receptor 1 (MCH1[145]), neurokinin 1 receptor (NK1R[143]), oxoeicosanoid receptor (OXER1[171]), P2Y purinoceptor 1 (P2RY1[175]) and transferrin receptor 1 (TRFR1[180]). The maximum heavy atom count of FPR1[153] is not shown for clarity purposes. Only hits for which: i) binding affinity K_i/IC_{50}/EC_{50}/K_B ≤ 15 μM was experimentally determined; and ii) for which a molecular structure was reported, are included in the analysis. The affinity of the OXER hit compound was not quantified[171] and is therefore only included in A.

2.3 *In silico* guidance: Optimization of Virtual Screening Hits

The identification of active compounds for a specific target using VS is only the first step in the search for novel leads with the targeted affinity, selectivity and/or pharmacological properties and is often followed by SAR exploration, site-directed mutagenesis studies and structure-guided optimization. True rational prospective structure-based hit optimizations, however, remain relatively scarce.[190, 191] Nevertheless some of the new hits identified in GPCR structure-based virtual screening campaigns (Table 2.2) have been optimized to improve ligand affinity,[145, 181] receptor selectivity,[159, 167, 192] pharmacokinetic properties,[167] and to explore SAR to validate predicted binding modes.[146, 169, 180, 193] Some of these hit optimization studies have been driven by structure-based design.[159, 167, 169, 192, 193]

One of the most frequently observed steps in a VS hit exploration is the search for close analogues of one or more hit compounds[157-159, 172, 194] or to synthesize a small series around one or more hit compounds[175, 189] (Table 2.2). The experimental validation of compound **8**, an $A_{2A}R$-selective VS hit from Carlsson et al.,[158] was followed by an analogue search which yielded 5 equally selective analogues but all with a lower affinity. Langmead et al.[159] also performed an analogue search for one of their $A_{2A}R$ structure-based virtual screening hits (cpd. **9a**). This search yielded three interesting analogues, amongst them was a selective (16-fold over A_1R) and highly potent (pK_i = 8.5) compound (**9b**) and an even more selective (>100-fold over A_1R) but slightly less potent (pK_i = 7.8) compound. Compound **10a**, the compound with the highest LE (LE of 0.53, see Figure 2.3b), and a chromone-containing compound were also further investigated with a ligand deconstruction study and a hit-to-lead synthesis program.

The SAR obtained from the deconstruction of compound **10a** highlighted that the phenol in combination with the amino functionality was the core scaffold for high potency ligands. Subsequently the propenyl-thiophene was reduced to an isopropyl, which yielded a simplified compound with only 17 heavy atoms and a pK_i of 7.9 (resulting in a LE of 0.64). Further substitutions yielded amongst others a highly potent (pK_i = 9.0) and highly selective (59-fold over A_1R) compound (**10b**) by introducing a *N*-methylpiperazine moiety. Optimization of these triazine compounds (**10a** and **10b**) was continued in a rational structure-based optimization study.[167, 168] Instead of 1,3,5-triazines derivatives, 1,2,4-triazine derivatives were further explored by combined SPR, SDM, *in silico* binding mode studies and *in silico* thermodynamic stability calculations of water molecules. Three of the designed compounds (**11a**, **11b** and **11c**) were also successfully crystallized in $A_{2A}R$ and corroborated the modeling approach.[167, 168] Also the proposed binding mode of the β_2R antagonist **17**, discovered by β_2R crystal structure-based *in silico* screening[164] was later experimentally validated by a co-crystal structure of β_2R and **19** (PDB-code: 3NY9).[193]

The SBVS study performed by Carlsson et al. against both a homology model and a crystal structure yielded 11 new compounds. The compound with the most novel scaffold (compound **17a**) was further explored by the purchase of 20 analogues. Most of the analogues showed the submicromolar affinity for D_3R and (sub)micromolar affinity for D_2R. The 2,5-dichlorophenyl derivatives appeared to have a slight selectivity towards D_3R over D_2R in contrast to the 3,5-dichlorophenyl derivatives as they showed comparable affinity towards both receptors. Reduction of the 2-methylpropane-1,3-diol tail into a 2-methylpropane-1-ol (**17b**) and a methyl (**17c**) yielded submicromolar affinity compounds (for D_2R and D_3R) with high ligand efficiencies (LE of 0.38, 0.47 and 0.57 for **17a**, **17b** and **17c** respectively).

Lin et al.[169] discovered that the kinase-inhibitor sorafenib (**36**) is also a 5-HTR antagonist based on a SBVS study against a 5-HT_{2A}R homology model. Based on the predicted binding mode of sorafenib in 5-HT_{2A}R multiple analogues were designed and two of them were synthesized to further validate this surprising discovery. The replacement of the aromatic nitrogen with a carbon slightly improved the binding affinity indicating that this atom was not engaged in a polar interaction with the receptor. However, the subsequent addition of a methyl group on the nitrogen atom of the amide resulted in a more than 9-fold loss of affinity which again indicated that the hypothesized binding mode was correct in which this nitrogen was engaged in hydrogen bonding with $L^{7.35}$.

Kim et al.[172] obtained a comparably surprising result in their SBVS study against a CXCR4 homology model in which one hit (**39a**) was identified that was very closely related to known anti-malarial drugs. The obvious next step was to also test these compounds (chloroquine (**39b**), hydroxychloroquine and quinacrine) and they were all found to be active against CXCR4. Apparently the replacement of the methoxy moiety with a chlorine atom (the sole difference between hit compound **39a** and anti-malarial drug chloroquine **39b**) did not have a significant impact of the affinity and cell migration, thereby opening up new repurposing possibilities for anti-malarial drugs.

The most potent of the three hits (compound **49**) from the structure-based pharmacophore screen against $P2Y_1$R was explored by both the purchase of commercially available analogues as well as the synthesis of multiple analogues. Synthesis of the analogues focused on the redecoration of the phenyl ring (from the 3,4-dichlorophenyl moiety in **49**) with different substituents on all positions. However, all synthesized analogues showed a lower binding affinity as well as lower inhibition of the Ca^{2+} efflux than hit **49**. Moreover, the replacement of the chlorine atoms with fluorine atoms or a methoxy moiety resulted in the complete loss of binding affinity for $P2Y_1$R. Two analogues that were purchased contained different substituents for the 3,4-dimethylisoxazole moiety of hit **49**, and had a slightly higher binding affinity (K_i = 6-10 μM) than the initial hit (13 μM).[175]

Tosh et al.[195] optimized adenosine 5′-carboxamide derivatives for A_{2A}R by combining binding mode predictions with *in silico* fragment replacement and redocking techniques. The initial binding modes of some adenosine 5′-carboxamide derivatives suggested optimization of these compounds towards $W^{6.48}$. By manual fragment replacement several optimizations were proposed and an automated fragment replacement resulted in 2000 proposals. The proposed compounds were energy optimized in the binding pocket from which the top 100 compounds were selected for redocking and rescoring. 23 compounds were subsequently selected and synthesized for further testing. This resulted in 2 inactive compounds and 22 compounds with highly differing affinity and selectivity profiles, but most of them had submicromolar affinity for A_{2A}R and were full or partial agonists at A_1R.

The overview in Figure 2.3a shows that several of the GPCR ligands identified in SBVS campaigns are relatively small (≤ 22 heavy atoms), this offers new possibilities for a fragment-based drug design approach. In fact, in the first SBVS study against the H_1R[161] crystal structure successfully retrieved many novel ligands with good ligand efficiency[196] (LE) from a library of fragment-like molecules (incl. **23** (LE=0.57), **24** (LE=0.45) and **25** (LE=0.44)).[161] Also SBVS runs against, for example, A_{2A}R have resulted in fragment-like hits[163] with good ligand efficiency (9 hits with LE between 0.3 and 0.5 incl. **7** (LE = 0.34)). It should be noted, however, that structure-based optimization of fragments can be challenging because small fragments can adopt a larger variety

of binding modes in different protein (sub)pockets.[197, 198] Furthermore scoring functions used to estimate the binding affinity and determine binding modes in molecular docking simulations are not trained for ranking (the poses of) small fragment-like compounds.[45, 51, 198] Virtual fragment screening with a molecular interaction fingerprint (IFP[45, 51]) is a suitable alternative approach to select ligands that can make specific interactions in specific binding pockets.[122, 161, 162] Validated fragments can then efficiently be used as starting points for ligand optimization strategies by fragment growing, linking, or merging[8, 198] of fragments originating from different IFP ranking lists.

2.4 Exploring novel GPCR-ligand interaction space in more detail

The presented overview shows that structure-based GPCR ligand discovery is growing in popularity and success. Many virtual screening studies have resulted in the discovery of novel ligands for diverse class A GPCRs and recently also the first class B SBVS has been reported.[122] As opposed to the more recent computer-aided ligand discovery and design studies, previous studies were mostly focused on the identification of larger ligands (Figure 2.3a). However, the focus is currently gradually shifting towards smaller ligands (fragments) with high ligand efficiency.[161, 163, 196] This fragment-based drug discovery approach[9] is starting to have an impact on the targeted compounds in SBVS studies, as the average heavy atom count of the obtained ligands is decreasing (Figure 2.3a) and simultaneously their ligand efficiency is increasing (Figure 2.3b). Several discussed studies have demonstrated that insights in GPCR-ligand interactions obtained from combined experimental and *in silico* modeling techniques can be used to enable fragment-based drug discovery and design against GPCRs.[150, 161, 170] Despite this progress, the sometimes low affinity of small fragments can be a problem as the difference in size of the endogenous ligands between GPCRs (e.g. neurotransmitters versus chemokines) influences the shape of the orthosteric binding pocket and thereby its recognition of fragments-like ligands.[8] Therefore a thorough retrospective validation is *pivotal* for a successful SBVS for fragment-like molecules, which emphasizes the need for GPCR-target annotated fragment libraries with true actives *and* true inactives.[9]

The increasing number of GPCR crystal structures[176] has brought a wealth of detailed structural insights into the molecular recognition mechanisms of (small) ligands. This has opened up new possibilities for (high resolution) homology modeling as they facilitate better templates and insights in regions with relatively high structural variability (e.g. extracellular loops) as well as the structural features of sequence-specific motifs (e.g. the helical kink induced by the TXP motif in CXCR4).[100] The new GPCR crystal structures in combination with molecular dynamics simulations give insights into receptor flexibility and (potential) ligand access and exit channels.[111, 199, 200] The association and dissociation pathways revealed by computational simulations in combination with experimental studies (e.g. mutagenesis data and biophysical measurements[167]) can in time be used to relate ligand structure to kinetic properties, thereby changing the focus from solely affinity-based optimizations to optimization of kinetic properties.[201, 202] Ultimately, a better understanding of the ligand binding modes,[203] binding pockets,[204] and conformational changes[205, 206] associated with (specific) signaling pathways will allow the development of selective SBVS strategies for agonists over antagonists (or *vice versa*) or ultimately even for *biased* ligands.